Forschungszentrum Karlsruhe
in der Helmholtz-Gemeinschaft

Wissenschaftliche Berichte
FZKA 7028

On Origin of Super-rotating Tangential Layers in Magnetohydrodynamic Flows

L. Bühler

Institut für Kern- und Energietechnik
Programm Kernfusion

August 2004

Forschungszentrum Karlsruhe

in der Helmholtz-Gemeinschaft

Wissenschaftliche Berichte

FZKA 7028

On origin of super-rotating tangential layers in magnetohydrodynamic flows

L. Bühler

Institut für Kern- und Energietechnik
Programm Kernfusion

Forschungszentrum Karlsruhe GmbH, Karlsruhe
2004

Impressum der Print-Ausgabe:

Als Manuskript gedruckt

Forschungszentrum Karlsruhe GmbH
Postfach 3640, 76021 Karlsruhe

Mitglied der Hermann von Helmholtz-Gemeinschaft
Deutscher Forschungszentren (HGF)

ISSN 0947-8620

urn:nbn:de:0005-070288

On origin of super-rotating tangential layers in magnetohydrodynamic flows

Abstract

An asymptotic analysis for magnetohydrodynamic flows between perfectly conducting concentric cylindrical shells has been performed. The flow in the model geometry exhibits all features which had been discovered in the past for the case of differentially rotating spherical shells considered in the context of geophysical analyses. For strong magnetic fields the flow region splits into distinct subregions and exhibits two different types of cores which are separated from each other by a tangent shear layer. The fluid in one core flows similar to a solid-body rotation and the outer core is entirely stagnant. For stronger magnetic fields the shear layer becomes thinner and since the flow rate carried by the layer asymptotes to a finite value the velocity in the layer increases as the layer thickness decreases. Moreover, the flux carried by the layer rotates in the opposite direction compared with the rotation of the body. It is shown that the rotating jet is driven by the electric potential difference between the edges of the inner and the outer core.

The considered tangent layer is very similar to the internal layers observed in pressure driven 3D MHD flows through ducts with sharp expansions. Such flows received attention in nuclear fusion engineering as e.g. described in Bühler (2003), technical report, Forschungszentrum Karlsruhe, FZKA 6904. While in the case of 3D duct flows the core solutions have to be determined numerically, in the present example of a rotating flow, the core solutions are known analytically. For that reason the rotating layer served as a test example for the derivation of the more complex flows described in the latter reference.

Zur Entstehung schnell-rotierender tangentialer Scherschichten in magnetohydrodynamischen Strömungen

Zusammenfassung

Magnetohydrodynamische Strömungen im Zwischenraum zweier perfekt leitender konzentrischer Zylinder werden mittels asymptotischer Rechnungen analysiert. Die Strömung in dieser Modellgeometrie weist alle Eigenschaften auf, die bei rotierenden magnetohydrodynamischen Strömungen in einem Kugelspalt zu beobachten sind. Derartige Strömungen sind zum Beispiel Gegenstand geophysikalischer Forschung. Für starke Magnetfelder entstehen im Fluid typische Strömungsgebiete. Man findet zwei unterschiedliche Kernströmungsbereiche, die durch eine tangentiale Scherschicht voneinander getrennt sind. Die Strömung im inneren Kern ist vergleichbar mit einer Starrkörperrotation und der äußere Kern bewegt sich praktisch nicht. Mit zunehmendem Magnetfeld wird die Scherschicht dünner. Da der Volumenstrom innerhalb der Schicht gegen einen endlichen Wert strebt, ergeben sich zunehmend größere Geschwindigkeiten, je dünner die Scherschicht wird. Darüber hinaus bewegt sich das Fluid in der Schicht vornehmlich entgegen der Rotationsrichtung des inneren Zylinders. Der Antrieb der schnell-rotierenden Schicht erfolgt aufgrund einer Differenz der elektrischen Potentiale zwischen der inneren und äußeren Kernströmung.

Die betrachtete tangentiale Schicht ähnelt den internen Scherschichten, die bei dreidimensionalen Druck-getriebenen MHD Strömungen in Kanälen mit abrupten Querschnittsänderungen auftreten. Solche Strömungen sind in der Fusionsforschung von Interesse; siehe z.B. Bühler (2003), Bericht, Forschungszentrum Karlsruhe, FZKA 6904. Während für 3D Kanalströmungen die Kernlösungen nummerisch bestimmt werden müssen, sind diese Lösungen im vorliegenden Problem analytisch bekannt. Deshalb diente die rotierende Schicht als Testbeispiel für die Herleitung der komplizierteren Strömung des zuvor genannten Berichts.

On origin of super-rotating tangential layers in magnetohydrodynamic flows

Contents

1 Introduction

In a recent paper Hollerbach and Skinner (2001) analyze the flow between differentially rotating concentric conducting spheres (fixed outer sphere) in a coaxial uniform magnetic field. They find by numerical techniques a shear layer at the edge of the inner sphere that spreads along magnetic field lines, i.e. along the so-called tangent cylinder. The latter authors "discovered accidentally" a high-velocity jet in the layer which has an opposite sense of rotation compared with the sphere and they relate the maximum of the jet velocity to be proportional to $Ha^{0.6}$. The thickness of the layer decreases with increasing magnetic field, given by the non-dimensional quantity, the Hartmann number Ha. The shear layer is called here the tangent layer although throughout the MHD literature such layers are often referred to as parallel layers.

In the following we give the physical explanation for this jet, and the asymptotic scaling law for the velocity for the case of high Hartmann numbers. In order to get insight into the physical phenomena we consider a modified geometry that allows for simpler mathematical treatment. We consider a cylindrical container in which a perfectly conducting smaller coaxial cylinder is rotating at uniform angular velocity. The Original geometry used by Hollerbach and Skinner (2001) and the model geometry used here are shown in Fig. 1. The rotating body has a non-dimensional radial extension $r = 1$ and an axial length $2Z_c$. The outer shell or the container has an axial extension up to $2Z_C$. The flow in the present geometry exhibits all features of Hollerbach and Skinner's problem namely a rotating inner core I, a stagnant outer core II, and a shear layer that separates both cores. The model geometry allows for efficient asymptotic analysis. The equations simplify to such a form that they can be solved analytically and provide a basis for understanding the numerical observations. Integration of the velocity profile becomes possible and the flow rate carried by the jet in the shear layer can be determined in closed form.

Theoretical studies on unbounded MHD flows initiated by rotating obstacles have been published e.g. by Antimirov and Molokov (1989) or Molokov (1993) without any indication of counter rotation. So we conclude that counter rotation is initiated by the rotation of conducting bodies in a domain of finite extension, bounded by conducting walls. It is further worth to note that flows driven by rotating cylinders and rings has been investigated already by Lehnert (1952) and Lehnert (1956). Due to different electric boundary conditions compared with the present cases, however, counter rotation could not be observed in those experiments.

It should be mentioned that the present type of tangential layer has much in common with the internal expansion layer which occurs in three-dimensional pressure-driven MHD flows at sharp geometric expansions. Such flows have been mentioned e.g. in the report by Bühler (2003) in applications for nuclear fusion reactors. While in such flows the core solutions must be determined numerically, in the present case of axisymmetric rotation, the core solutions are known analytically. Moreover, the variables here do not change in circumferential direction while in the case of 3D duct flows the layer variables change not only along field lines but also along both transverse directions. For that reason the rotating layer considered here is somehow simpler compared with the expansion layer and it served as a test example for the derivation of the more complex flows mentioned by Bühler (2003).

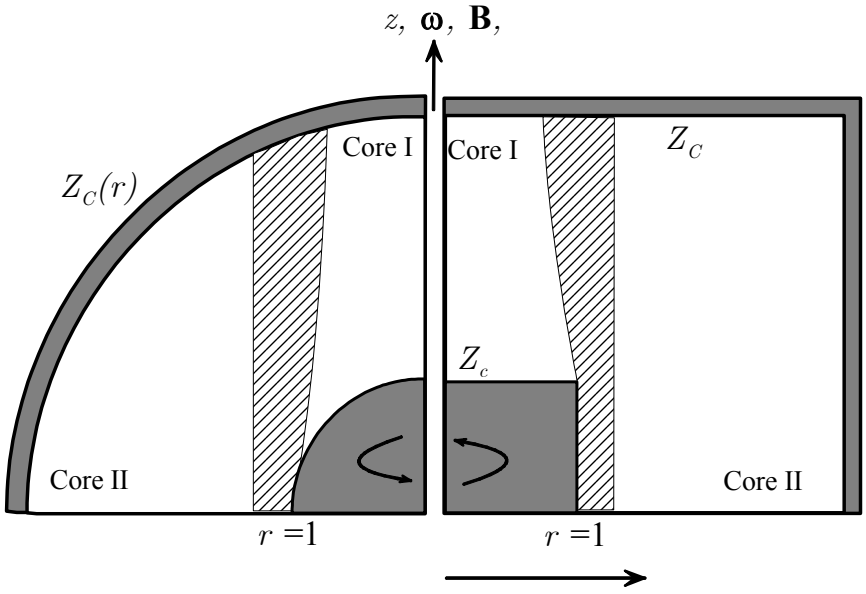

Figure 1: Sketch of the spherical annulus as used by Hollerbach and Skinner (2001) (left). The outer sphere is fixed and the inner sphere rotates at uniform angular velocity around the z axis. Sketch of a cylinder of finite length Z_c rotating in a fluid confined in a cylindrical vessel (right). In both geometries tangent layers evolve at $r = 1$ and spread along magnetic field lines. The plane $z = 0$ is a symmetry plane

2 Formulation

Consider the inductionless magnetohydrodynamic flow of an incompressible viscous fluid, governed by the balance of momentum

$$\frac{1}{N}\frac{d\mathbf{v}}{dt} = -\nabla p + \frac{1}{Ha^2}\nabla^2\mathbf{v} + \mathbf{j}\times\mathbf{B}, \tag{1}$$

and by Ohm's law

$$\mathbf{j} = -\nabla\phi + \mathbf{v}\times\mathbf{B}, \tag{2}$$

with conservation of mass and charge

$$\nabla\cdot\mathbf{v} = 0, \quad \nabla\cdot\mathbf{j} = 0. \tag{3}$$

At the fluid wall interface the flow has to satisfy the no-slip condition

$$\mathbf{v} = \mathbf{v}_w, \tag{4}$$

and continuity of electric potential (no contact resistance)

$$\phi = \phi_w. \tag{5}$$

The subscript w denotes properties at the walls. In the equations shown above $\mathbf{v}$, $\mathbf{B}$, $\mathbf{j}$, p, ϕ stand for velocity, magnetic induction, current density, pressure and electric potential, scaled by the reference quantities v_0, B_0, $j_0 = \sigma v_0 B_0$, $\sigma v_0 B_0^2 L$ and $v_0 B_0 L$, respectively. The scale of velocity is v_0 and L is a typical length scale, e.g. the radius of the rotating body. The quantity B_0 is the magnitude of the applied magnetic induction. The fluid properties like the electric conductivity σ, the kinematic viscosity ν, and the density ρ, are assumed to be constant. The inductionless equations shown above apply for flows with moderate velocities and dimensions. To be more precise for flows with small magnetic Reynolds numbers $R_m = \mu\sigma v_0 L \ll 1$. Here μ stands for the magnetic permeability. For such conditions the disturbance of the applied magnetic field by the flow is negligible.

The flow is governed by two nondimensional parameters, the Hartmann number Ha and the interaction parameter N

$$Ha = B_0 L\sqrt{\frac{\sigma}{\rho\nu}}\,, \qquad N = \frac{\sigma L B_0^2}{\rho v_0}\,. \tag{6}$$

The square of the Hartmann number characterizes the ratio of electromagnetic forces ($\sigma v_0 L B_0^2$) to viscous forces ($\rho\nu v_0/L$) while the interaction parameter represents the ratio of electromagnetic forces to inertia forces (ρv_0^2).

For many problems it is suitable to eliminate pressure by taking the curl of the momentum equation using the vorticity $\boldsymbol{\omega} = \nabla\times\mathbf{v}$. This yields in the inertialess limit as $N\to\infty$

$$\frac{1}{Ha^2}\nabla^2\boldsymbol{\omega} + (\mathbf{B}\cdot\nabla)\,\mathbf{j} = 0. \tag{7}$$

With increasing interaction parameter, the influence of inertia decreases and therefore the secondary motion induced by centrifugal acceleration becomes negligible. It has been shown by Fidaros (2004) that for $N \gg 100$, secondary motions are so small that their influence on the circumferential flow is practically absent so that the inertialess assumption used here is justified.

If we use charge conservation (3) in Ohm's law we find an equation for electric potential ϕ as

$$\nabla^2\phi = \nabla \cdot (\mathbf{v} \times \mathbf{B}) = \mathbf{B} \cdot \boldsymbol{\omega}. \tag{8}$$

In the following we focus on the flow confined in an axisymmetric container in which a submersed solid body is rotating at constant vorticity $\boldsymbol{\omega}_b = 2\hat{\mathbf{z}}$ around the symmetry axis of the device. We assume that the computational domain is penetrated by an externally applied uniform magnetic field $\mathbf{B} = \hat{\mathbf{z}}$. The governing equations then reduce for the axial component of vorticity $\omega = \boldsymbol{\omega} \cdot \hat{\mathbf{z}}$ and for potential ϕ to

$$\frac{1}{Ha^2}\nabla^2\omega = -\partial_z j_z = \partial_{zz}\phi, \tag{9}$$

$$\nabla^2\phi = \omega. \tag{10}$$

We may eliminate ω from these equations and find a single equation for potential

$$\frac{1}{Ha^2}\nabla^4\phi = \partial_{zz}\phi, \tag{11}$$

or we may eliminate ϕ and find a single equation for vorticity as

$$\frac{1}{Ha^2}\nabla^4\omega = \partial_{zz}\omega. \tag{12}$$

These equations for the fluid are exact in the inertialess limit as $N \to \infty$.

Note that for axisymmetric applications, where $\mathbf{v} = v\hat{\boldsymbol{\varphi}}$, the axial vorticity is related to circumferential velocity v according to

$$\omega = \frac{1}{r}\partial_r (rv). \tag{13}$$

For determining velocity from potential we introduce (13) in (10) and find

$$\frac{1}{r}\partial_r (r\partial_r\phi) + \partial_{zz}\phi = \frac{1}{r}\partial_r (rv). \tag{14}$$

The velocity v is obtained by integration once the potential has been determined.

In the following we consider the flow in a cylindrical container of non-dimensional height $2Z_C$, in which a perfectly conducting solid cylinder is rotating. The rotating cylinder has a non-dimensional radius of one and an extension along the axis of $2Z_c$. The geometry is sketched in Fig. 1.

Let us consider first the equations for the solid body, rotating with $\boldsymbol{\omega}_b = 2\hat{\mathbf{z}}$ in a magnetic field $\mathbf{B} = \hat{\mathbf{z}}$. The solid body rotation is prescribed by a single component of velocity with $v = r$. For highly conducting bodies, Ohm's law reduces to

$$\nabla\phi_b = v\hat{\boldsymbol{\varphi}} \times \hat{\mathbf{z}} = v\hat{\mathbf{r}}, \tag{15}$$

and we find for the potential ϕ_b of the rotating body that

$$\partial_r \phi_b = v = r. \tag{16}$$

The potential finally has a solution

$$\phi_b = \frac{1}{2} r^2 + \phi_0, \tag{17}$$

where ϕ_0 is an integration constant.

3 Core solution

For strong magnetic fields the viscous effects are confined to very thin boundary or internal layers and almost all the fluid domain behaves as being inviscid. The inviscid flow occurs in two different types of cores. One is above and below the rotating body for $r < 1$, the other one is outside the tangent cylinder for $r > 1$. The problem in the cores simplifies for $Ha \to \infty$ to

$$\partial_{zz}\phi = 0, \tag{18}$$

$$\omega = \nabla^2 \phi. \tag{19}$$

This means that we may determine the potential ϕ of the inviscid solution by integration of (18), once the values at the boundaries are known. At the interface to the rotor we know ϕ already from (17)

$$\phi = \phi_b + O\left(Ha^{-2}\right) \quad \text{at } z = Z_c \tag{20}$$

and if the outer wall is a perfect conductor we have there

$$\phi = 0 + O\left(Ha^{-2}\right) \text{ at } z = Z_C \tag{21}$$

without loss of generality. The viscous corrections for potential due to the Hartmann layers are as small as $O\left(Ha^{-2}\right)$ according to Moreau (1990) or other text books on MHD flows. For that reason we may neglect these contributions for potential and apply directly the conditions at the walls to the core variables. Here and in the following the subscripts c and C denote variables in the inner and outer cores, respectively (see e.g. Fig 1).

The potential and the vorticity in the fluid that satisfy the core equations and boundary conditions read now:

$$\left.\begin{aligned} \phi_c &= \left(\tfrac{1}{2} r^2 + \phi_0\right) \tfrac{Z_C - z}{Z_C - Z_c} \\ \omega_c &= \nabla^2 \phi_c = 2 \tfrac{Z_C - z}{Z_C - Z_c} \end{aligned}\right\} \text{ for } r < 1, \tag{22}$$

and

$$\left.\begin{aligned} \phi_C &= 0 \\ \omega_C &= 0 \end{aligned}\right\} \text{ for } r > 1. \tag{23}$$

Conservation of charge for the rotating body requires that the integral current that enters and leaves the rotor vanishes. This leads to the condition that

$$\int_0^1 \partial_z \phi_c \, 2\pi r \, dr = 0. \tag{24}$$

This equation determines the yet unknown potential ϕ_0 on the axis of the rotor to

$$\phi_0 = -\frac{1}{4}. \tag{25}$$

A key feature of the current problem is that the core solution for ω satisfies already the boundary conditions for the viscous problem. This means that there are no Hartmann layers at the walls, even if the magnetic field has a non-zero component normal to the boundaries. A viscous correction near Hartmann walls is therefore not necessary. This is a result of the assumption that walls and rotor are perfect conductors. In case of finite conductivity of these walls Hartmann layers would appear and a viscous correction in these layers would be necessary.

The velocity in the cores is obtained by integration of vorticity according to the equation (13). We find for the inner core

$$v_c = r\frac{Z_C - z}{Z_C - Z_c} \quad \text{for } r < 1, \tag{26}$$

and for the outer one

$$v_C = 0 \quad \text{for } r > 1. \tag{27}$$

If we compare the core solutions in both cores we realize that they are discontinuous across the tangent cylinder at $r = 1$. We find jumps of

$$\tfrac{1}{2}\,[\omega] = [v] = 4\,[\phi] = \begin{cases} \frac{Z_C - z}{Z_C - Z_c} & \text{for} \quad Z_c < z < Z_C \\ 1 & \text{for} \quad 0 < z < Z_c \end{cases}, \tag{28}$$

where [ ] stands for the difference of a core quantity between $r = 1 - \varepsilon$ and $r = 1 + \varepsilon$.

To complete the discussion for the cores we evaluate the electric currents.

$$j_r = -\partial_r \phi + v, \tag{29}$$

$$j_\varphi = 0, \tag{30}$$

$$j_z = -\partial_z \phi. \tag{31}$$

Using core solutions for ϕ and v we obtain

$$\begin{aligned} j_r = j_\varphi = 0,\ j_z = \tfrac{\frac{1}{2}r^2 - \frac{1}{4}}{Z_C - Z_c} \quad \text{for} \quad r < 1, \\ j_r = j_\varphi = \ j_z = 0, \qquad \text{for} \quad r > 1. \end{aligned} \tag{32}$$

As a result we find that the core currents flow exclusively along magnetic field lines. The same result has been obtained numerically by Hollerbach and Skinner (2001) for the flow in a spherical annulus. As a consequence, Lorentz forces are absent. Deviations from this behavior occur only in regions where viscous effects are important, i.e. in the viscous layer in the vicinity of the tangent cylinder. This topic will be discussed in the following sections.

4 The tangent layer

For high Hartmann numbers the shear layer along the tangent cylinder is very thin, $\delta \ll 1$. The behavior inside the layer allows therefore for an analysis using locally Cartesian coordinates with a stretched layer-normal coordinate

$$x = \frac{r-1}{\delta}. \tag{33}$$

Let us consider the potential equation (11) in stretches coordinates. We consider in the Laplace operator only the leading order terms in δ. This gives the separable equation

$$\frac{1}{Ha^2}\frac{1}{\delta^4}\partial_x^4\phi = \partial_{zz}\phi, \tag{34}$$

and a reasonable balance between viscous and Lorentz forces requires that

$$\delta = Ha^{-1/2}. \tag{35}$$

This simplifies the potential equation to

$$\partial_x^4\phi = \partial_{zz}\phi. \tag{36}$$

Note, the simplified equation in stretched coordinates implies that the radial current density does not change at leading order of approximation through the layer. A viscous correction for layer-normal current density in the Ohm's law is not present and the viscous corrections for velocity and potential are related simply as

$$v_t = \sqrt{Ha}\partial_x\phi_t, \tag{37}$$

where v_t and ϕ_t stand for the viscous corrections to the core solution in the tangent layer, i.e.

$$\left.\begin{array}{c}\phi = \phi_c + \phi_t \\ v = v_c + v_t \\ \omega = \omega_c + \omega_t\end{array}\right\} \quad \text{for } x < 0, \tag{38}$$

where ϕ_c, v_c, ω_c are the inner core solution at $x = 0$, $(r = 1)$.

In the following we assume a viscous correction of potential inside the tangent layer of the type

$$\phi_t = \sum_{k=1}^{\infty} f_k(x)\sin\left(\beta_k\left(z - Z_c\right)\right), \tag{39}$$

in which $\beta_k = \frac{k\pi}{Z_C - Z_c}$ ensures correct boundary conditions at both perfectly conducting interfaces at $z = Z_c$ and $z = Z_C$. Substituted into the reduced potential equation (36) yields

$$\partial_x^4 f_k(x) + \beta_k^2 f_k(x) = 0. \tag{40}$$

General solutions that vanishes at sufficient distance from the layer are

$$f_k(x) = \left(a_k\cos\alpha_k x + b_k\sin\alpha_k x\right)\exp\left(\alpha_k x\right), \tag{41}$$

where $\alpha_k = \sqrt{\beta_k/2}$. The viscous corrections to velocity and vorticity become

$$v_t = \sqrt{Ha} \sum_{k=1}^{\infty} \partial_x f_k(x) \sin(\beta_k (z - Z_c)) \tag{42}$$

and

$$\omega_t = Ha \sum_{k=1}^{\infty} \partial_{xx} f_k(x) \sin(\beta_k (z - Z_c)). \tag{43}$$

Similarly we expand the solution outsider the tangent cylinder as

$$\left.\begin{array}{c} \phi = \phi_C + \phi_T \\ v = v_C + v_T \\ \omega = \omega_C + \omega_T \end{array}\right\} \text{ for } x > 0, \tag{44}$$

with

$$\phi_T = \sum_{K=1}^{\infty} F_K(x) \cos(\beta_K z), \tag{45}$$

$$v_T = \sqrt{Ha} \sum_{k=1}^{\infty} \partial_x F_K(x) \cos(\beta_K z), \tag{46}$$

$$\omega_T = Ha \sum_{k=1}^{\infty} \partial_{xx} F_k(x) \cos(\beta_K z), \tag{47}$$

where now

$$F_K(x) = (A_K \cos \alpha_K x + B_K \sin \alpha_K x) \exp(\alpha_K x), \tag{48}$$

with $\beta_K = \left(K - \frac{1}{2}\right) \pi / Z_c$ and $\alpha_K = -\sqrt{\beta_K/2}$. The solution satisfies correct boundary conditions at $z = Z_C$ and symmetry conditions at $z = 0$.

Matching of the solutions at $x = 0$, $(r = 1)$, provides enough conditions for the determination of the coefficients a_k and b_k and of the A_K and B_K. The details of the matching are outlined in the appendix.

To complete the analysis we consider integral quantities of the layer. It is possible to determine the amount of flow carried by the layer by an integration of the velocity profile. We find the flow rate carried in the upper half of the geometry as

$$\begin{aligned} Q &= Ha^{-1/2} \left(\int_{Z_c}^{Z_C} \int_{-\infty}^{0} v_t \, dx \, dz + \int_{0}^{Z_C} \int_{0}^{\infty} v_T \, dx \, dz \right) \\ &= -\int_{0}^{Z_C} [\phi] \, dz. \end{aligned} \tag{49}$$

The evaluation of the integrals gives

$$Q = -\frac{1}{8} (Z_C + Z_c), \tag{50}$$

and the total flow rate in just twice this value (upper and lower part of the geometry). We conclude that the amount of fluid carried by the tangent layer is an $O(1)$ quantity that

depends only on the geometry. Since the tangent layer has a thickness of $\delta \sim Ha^{-1/2}$ the corresponding velocities reach high magnitudes such as $v \sim Ha^{1/2}$. We further observe that the tangent layer rotates in opposite direction compared with the rotating inner cylinder.

5 Results

As an example we show the solution for potential and angular velocity driven by a perfectly conducting disc ($Z_c = 0$) rotating in a perfectly conducting cylindrical container as shown in Fig. 2 for a Hartmann number of $Ha = 100$. In fact, such low Hartmann numbers result in tangent layers which are relatively thick so that a basic assumption $\delta \ll 1$ is not perfectly satisfied and the present results could be inaccurate. Nevertheless it seems worth to show the figure since it may be compared with the calculations of Hollerbach and Skinner (2001) who use similar values of Ha. If we consider the variation of angular velocity we find a solid-body rotation near the center whose strength decreases towards the top wall of the container. The counter rotating flow reaches a magnitude of about $v/r = -1.1$. More closer to the geometry of a spherical shell is the

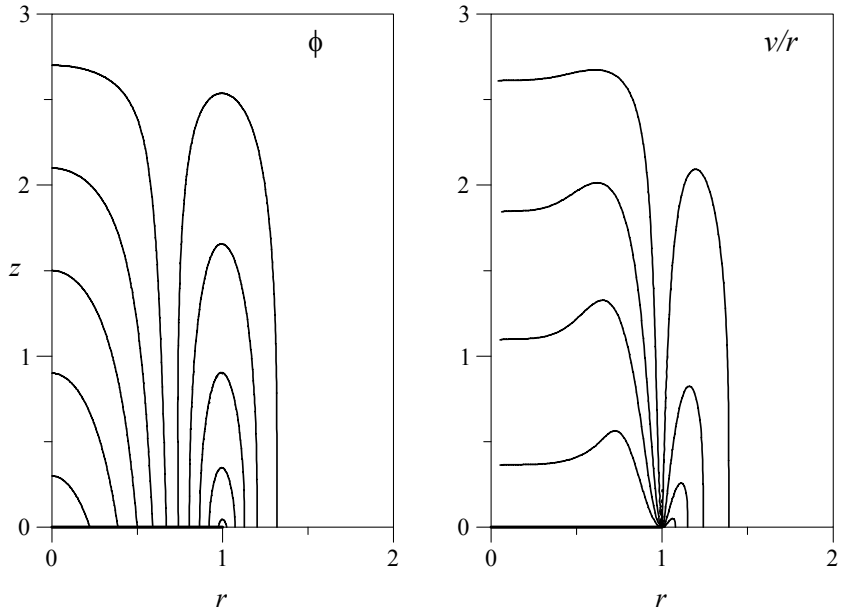

Figure 2: Contours of potential and angular velocity v/r in a t-layer, created by a perfectly conducting rotating disc at $Ha = 100$.

rotating cylinder with a finite length Z_c. As an example the flow driven by a rotating cylinder of length $Z_c = 1$ is shown in Fig. 3. Qualitatively the solution remains as for the rotating disc. We observe the inner core rotating as a solid body with decreasing magnitude along z, the stagnant outer core and a counter rotating jet in the tangent layer. The region inside the jet, where the velocity is high, extends now over a length that corresponds roughly to the elongation of the cylinder. This is the reason why the present jet carries a higher flow rate than the jet created by the rotating disc. For

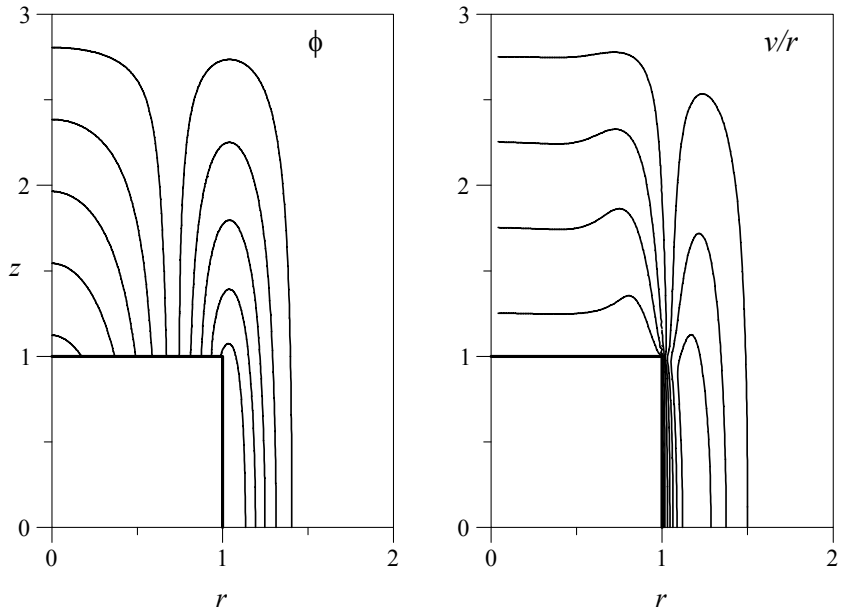

Figure 3: Contours of potential and angular velocity in a t- layer, created by a perfectly conducting rotating cylinder at $Ha = 100$.

increasing Hartmann numbers the tangent layer becomes thinner. This can be seen from Fig. 4, where the solutions for two different Hartmann numbers are compared. At the same time the magnitude of velocity increases as indicated by the larger number of isolines for $Ha = 1000$. Details in the layer, especially for the high Hartmann number case can be seen in Fig. 5, in which the solutions are plotted on stretched scales. We observe here that on this scale both solutions do not differ strongly besides the fact that there are more isolines due to the higher velocities for the case of higher Ha.

Let us consider now the magnitude of the reversed flow. It has been shown already that the flow rate carried by the tangent layer is

$$Q = -\frac{1}{8}\left(Z_C + Z_c\right). \tag{51}$$

The velocities related to such flow rates are on the order $Ha^{1/2}$. This behavior is plotted for the case of a rotating disc in Fig. 6. The radial coordinate is shown in stretched scale. We observe, as expected, an increase of the velocity magnitude as the Hartmann number increases. We find as suggested by our analysis the asymptotic behavior $v/r \sim Ha^{1/2}$ for high Hartmann numbers. In the lower range of investigated Hartmann numbers the solution scales slightly different. This has its origin in the fact that the jet velocity reaches same order of magnitude as the velocity of the counter rotating disc at which the no-slip condition has to be satisfied. By viscosity the disc tries to reduce the counter - rotating flow in the layer and to drive the flow in the direction of its own rotation. This effect must be responsible for the slightly lower values and for the small deviations from the asymptotic behavior. At higher Hartmann numbers the influence of potential wins upon viscous drag and establishes the asymptotic scaling law.

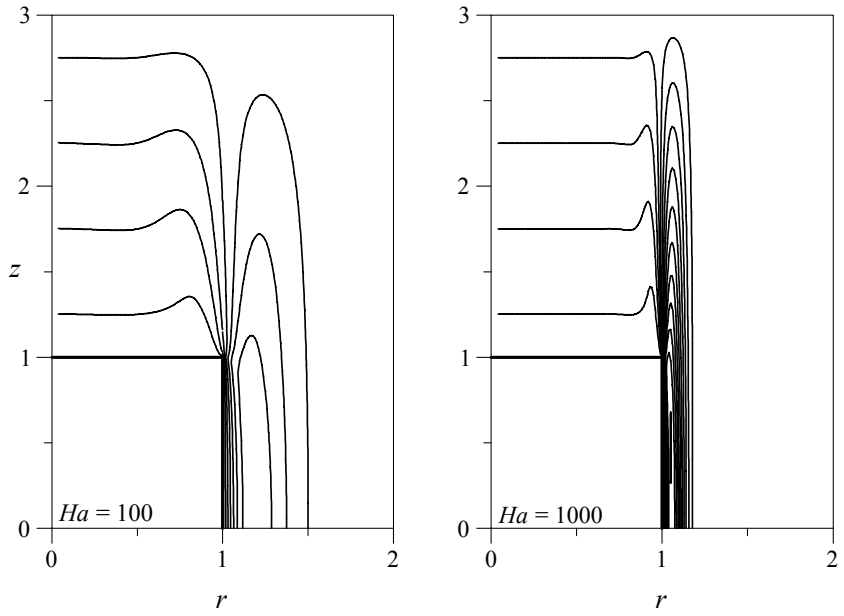

Figure 4: Contours of angular velocity v/r in a t- layer, created by a perfectly conducting rotating cylinder for two different Hartmann numbers.

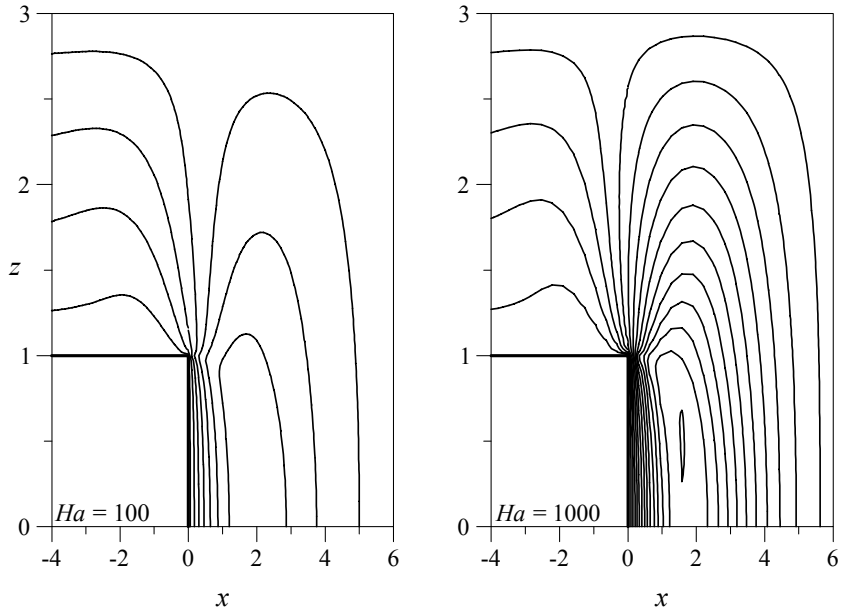

Figure 5: Contours of angular velocity in a t- layer, created by a perfectly conducting rotating cylinder for two different Hartmann numbers. The radial coordinate is shown in stretched scale.

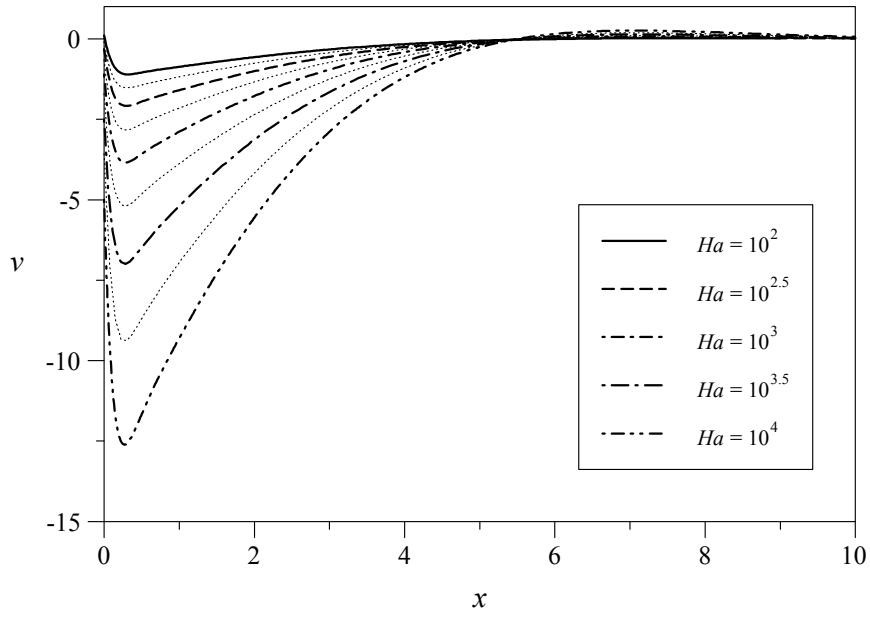

Figure 6: Velocity $v\,(x, z = 0)$ in the tangent layer for different Hartmann numbers

6 Spherical annulus

Now we apply the present analysis to the case of a spherical annulus as studied by Hollerbach and Skinner (2001). The solution for inner core potential remains similar to those shown before

$$\phi_c = \left(\frac{1}{2}r^2 + \phi_0\right)\frac{Z_C - z}{Z_C - Z_c} \quad \text{for } r < 1 \tag{52}$$

The upper and lower boundaries, however, are not constant any more, i.e. they depend on r as $Z_C = \sqrt{R^2 - r^2}$, and $Z_c = \sqrt{1 - r^2}$. The variable R stands here for the aspect ratio of the larger outer sphere compared with the inner one. For the special case compared later with literature, where $R = 3$, the potential at the axis evaluates as $\phi_0 = -0.23870$. Therefore the vorticity and velocity in the inner core get a more complicated representation since they are evaluated by derivatives of potential with respect to the radial direction r. Nevertheless, they are still known analytically. It has to mentioned that both, core velocity and vorticity become unbounded as $r \to 1$. In the closer vicinity to the tangent cylinder, the core solutions loose their physical relevance since there, the viscous corrections in the tangent layer become dominant. For that reason we evaluate the core velocity and vorticity only up the position $r = 1 - \delta$ and estimate core variables in $1 - \delta < r < 1$ by a linear extrapolation. All deviations from this behavior are accounted for in the viscous layer correction. It is further worth to notice, that the solutions for core velocity and vorticity do no longer satisfy the kinematic boundary conditions at Z_C and Z_c. This means that for the present case viscous Hartmann layers appear at these boundaries. Although these Hartmann layers do not contribute to the solution for potential (they do not carry an $O(1)$ integral current), they are required in order to satisfy no-slip at the walls. The solutions derived in this way for the tangent layer are valid except in a region where the layer meets the inner sphere. For a comparison of the present results with that obtained by Hollerbach and Skinner (2001) see Figs. 7 and 8. The qualitative agreement is quite good.

In Fig. **??** we see the dependence of the maximum jet velocity on the Hartmann number. We find again the asymptotic behavior $v/r \sim Ha^{1/2}$ for high Hartmann numbers. As a comparison the $Ha^{0.6}$ dependence proposed by Hollerbach and Skinner (2001) has been added to the figure for Hartmann numbers close to $Ha = 100$. This slope is approached by the present solution for the smaller Hartmann numbers investigated. The present solution has higher angular velocity than that derived by Hollerbach and Skinner (2001), a fact that may be attributed to the perfect conductance of the rotating body used here, while in the latter reference the sphere had a finite conductivity. This influence affects the solutions in in the cores and in the layer.

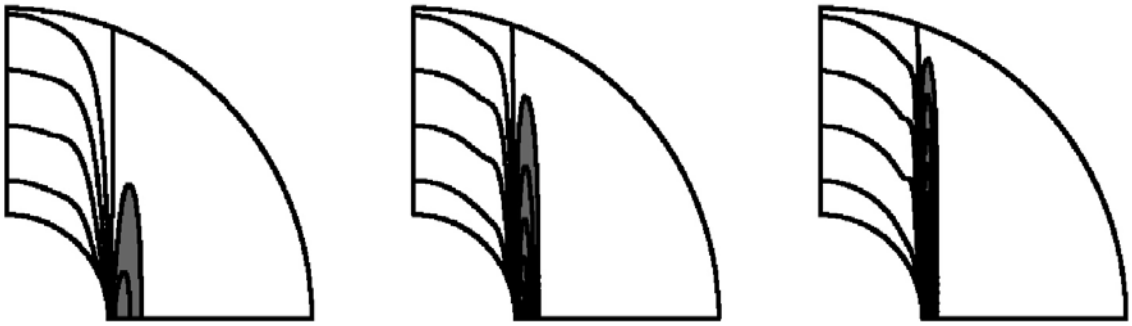

Figure 7: Contours of angular velocity in a spherical shell for $Ha = 10^2,\ 10^{2.5},\ 10^3$. The figure has been taken from Hollerbach and Skinner (2001).

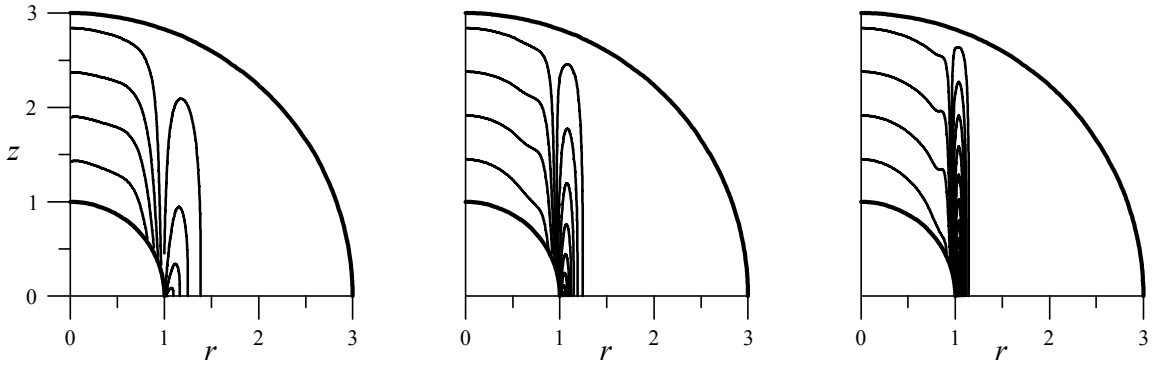

Figure 8: Contours of angular velocity in a spherical shell for $Ha = 10^2,\ 10^{2.5},\ 10^3$, present theory

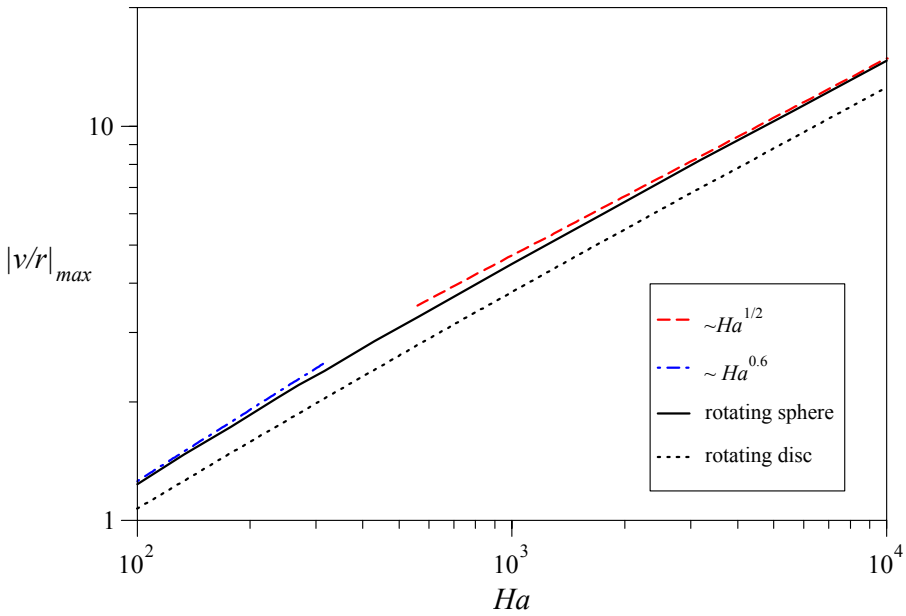

Figure 9: Asymptotic behavior of maximum jet velocities.

7 Hunt's flow

The present analysis shows that the jets that are mentioned by Hollerbach and Skinner (2001) are purely driven by the potential difference across the internal layer which separates both cores, the rotating and the stagnant one. The mass flux carried by the layer is directly proportional to this potential difference, integrated along the axial direction. The jet is present if such a potential difference exists, no matter how it is created, and independently of the rotation of the disc. One can imagine for example the case of two non-rotating discs on the top and bottom of an insulating container to which an external electric circuit is connected. Such a configuration has been considered first by Hunt and co-authors (1968-1970). These authors applied a certain voltage between the discs and found, for high Hartmann numbers, electrically driven rotating jet flows which were very similar to the ones observed for the case of rotating conducting bodies. Hunt's geometry is sketched in Fig.10. A first indication about the similarity of both types of flow has been given by Dormy, Jault and Soward (2002).

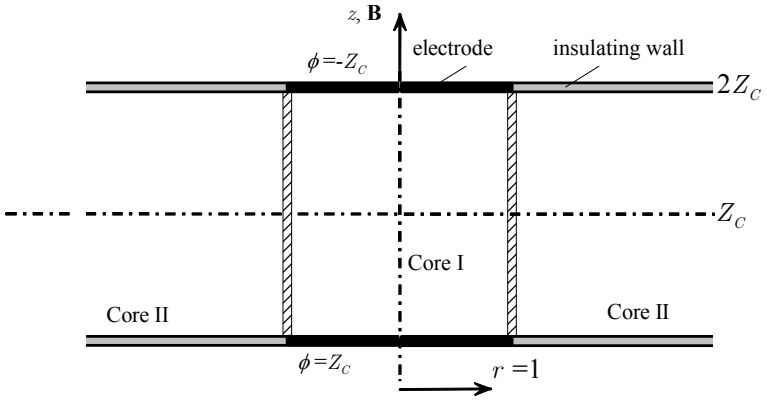

Figure 10: Sketch of the experiment performed by Hunt and Malcolm (1968).

Our present analysis applies perfectly to the latter case if one disc electrode is at $z = 0$, while $z = Z_C$ represents a symmetry plane. The core solutions take the form

$$v_c = 0,\ \phi_c = Z_C - z \text{ for } r < 1, \text{ and } v_C = \phi_C = 0 \text{ for } r > 1, \tag{53}$$

Therefore we have the no jump in core velocity but still a jump in potential as

$$[v] = 0, \quad [\phi] = Z_C - z. \tag{54}$$

The potential jump is directly proportional to the flow rate carried in the jet by the layer as shown in (49), i.e.

$$Q = -\int_0^{Z_C} [\phi]\ dz = -\frac{1}{2} Z_C^2. \tag{55}$$

One example for such jets is shown in Fig.11. This result agrees well with that derived by Hunt and Stewartson (1969) on the basis of a completely different analysis, if we take

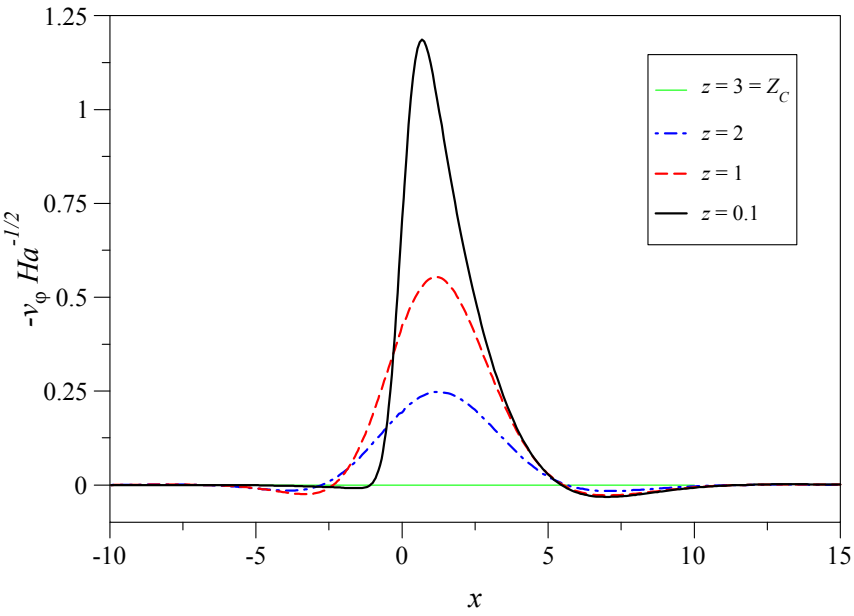

Figure 11: Circumferential velocity in the t-layer, driven by an applied voltage at conducting circular electrodes at a distance $2Z_C$ (compare Hunt and Malcolm (1968)).

into account that the present analysis uses different scales. The scale for velocity used here is chosen as $v_0 = \frac{U}{Z_C L B_0}$, where U is the dimensional potential difference between the bottom and the top electrode and Z_C is the non-dimensional aspect ratio. The dimensional quantity $\frac{U}{Z_C L}$ corresponds to the applied axial electric field.

8 Conclusions

An asymptotic analysis for concentric annular MHD flows has been performed. The flow in the model geometry allows for analytical treatment of the problem but exhibits all features which had been discovered in the past for the case of differentially rotating spherical shells. The analysis results in two different types of cores which are separated from each other by a tangent shear layer. One core is rotating at uniform vorticity, similar to a solid body rotation. At the rotor, the rotation rate of the flow is the same as that of the rotating body. The core vorticity, however, decays linearly along magnetic field lines and vanishes at the non-rotating walls. The outer core is entirely stagnant. For increasing Hartmann numbers the shear layer becomes thinner despite the fact that the flow rate carried by the layer asymptotes to an $O(1)$ finite value, which can be determined in closed form. As a result the velocity in the layer increases as the layer thickness δ decreases. Moreover, the flux carried by the layer rotates in the opposite direction compared with the rotation of the body. It is shown that the source of the rotating jet is the difference in electric potential between the edges of the inner and the outer core. This potential difference may be created by the electric field induced in the rotating conducting body as considered by Hollerbach and Skinner (2001) or it may be created if a certain voltage is applied at electrodes, independent of their rotation. In both cases similar tangent layers develop.

Concerning these facts it is not unexpected to observe high velocity jets in the case of rotating conducting bodies, "showing every sign of increasing indefinitely with" *Ha*. It would be of course interesting to observe such counter-rotating jets experimentally. It has to be mentioned, however, that for the equivalent case of conducting circular electrodes Hunt and Malcolm (1968) observed such jets experimentally so that there is no doubt that the phenomena described above exist.

A Appendix

A.1 Computational details

We have shown above that the solution in the tangent layer can be expanded in two different types of Fourier series, one valid for $x < 0$ and the other for $x > 0$. At $x = 0$ both solutions must match smoothly. This requires that

$$\phi_c + \sum_{k=1}^{\infty} a_k \sin\left(\beta_k \left(z - Z_c\right)\right) = \phi_C + \sum_{K=1}^{\infty} A_K \cos\left(\beta_K z\right) \text{ for } Z_c < z < Z_C, \quad (56)$$

$$\phi_c = \phi_C + \sum_{K=1}^{\infty} A_K \cos\left(\beta_K z\right) \text{ for } 0 < z < Z_c, \quad (57)$$

or

$$\sum_{K=1}^{\infty} A_K \cos\left(\beta_K z\right) = [\phi] + \begin{cases} \sum_{k=1}^{\infty} a_k \sin\left(\beta_k \left(z - Z_c\right)\right) & Z_c < z < Z_C \\ \text{for} & \\ 0 & 0 < z < Z_c \end{cases}, \quad (58)$$

which gives a first set of equations for the determination of the coefficients.

Matching of currents and velocity requires at $x = 0$ that

$$v_c + \sqrt{Ha} \sum_{k=1}^{\infty} \alpha_k \left(a_k + b_k\right) \sin\left(\beta_k \left(z - Z_c\right)\right)$$

$$= v_C + \sqrt{Ha} \sum_{K=1}^{\infty} \alpha_K \left(A_K + B_K\right) \cos\left(\beta_K z\right) \text{ for } Z_c < z < Z_C \quad (59)$$

$$v_c = v_C + \sqrt{Ha} \sum_{K=1}^{\infty} \alpha_K \left(A_K + B_K\right) \cos\left(\beta_K z\right) \text{ for } 0 < z < Z_c \quad (60)$$

This leads us to

$$\sum_{K=1}^{\infty} \alpha_K \left(A_K + B_K\right) \cos\left(\beta_K z\right)$$

$$= Ha^{-1/2} [v] + \begin{cases} \sum_{k=1}^{\infty} \alpha_k \left(a_k + b_k\right) \sin\left(\beta_k \left(z - Z_c\right)\right) & Z_c < z < Z_C \\ \text{for} & \\ 0 & 0 < z < Z_c \end{cases}. \quad (61)$$

Matching of vorticity gives equivalently

$$Ha^{-1} [\omega] + 2 \sum_{k=1}^{\infty} \alpha_k^2 b_k \sin\left(\beta_k \left(z - Z_c\right)\right) = 2 \sum_{K=1}^{\infty} \alpha_K^2 B_K \cos\left(\beta_K z\right) \text{ for } Z_c < z < Z_C. \quad (62)$$

Smooth solutions for vorticity further demand that

$$\sum_{k=1}^{\infty} \alpha_k^3 \left(a_k - b_k\right) \sin\left(\beta_k \left(z - Z_c\right)\right) = \sum_{K=1}^{\infty} \alpha_K^3 \left(A_K - B_K\right) \cos\left(\beta_K z\right) \text{ for } Z_c < z < Z_C. \quad (63)$$

We have finally a system of four equations for the four unknown a_k, b_k, A_K, B_K.

We use orthogonality of trigonometric functions to proceed and find

$$\frac{1}{2}Z_C A_K = \int_0^{Z_C} [\phi] \cos(\beta_K z)\, dz + \sum_{k=1}^{\infty} a_k \int_{Z_c}^{Z_C} \sin(\beta_k (z - Z_c)) \cos(\beta_K z)\, dz. \tag{64}$$

Using abbreviations

$$[\phi]_K = \frac{2}{Z_C} \int_0^{Z_C} [\phi] \cos(\beta_K z)\, dz \tag{65}$$

and

$$C_{kK} = 2 \int_{Z_c}^{Z_C} \sin(\beta_k (z - Z_c)) \cos(\beta_K z)\, dz \tag{66}$$

we arrive at

$$A_K = [\phi]_K + \frac{1}{Z_C} \sum_{k=1}^{\infty} a_k C_{kK}. \tag{67}$$

We proceed with velocities in the same way and find

$$\alpha_K (A_K + B_K) = Ha^{-1/2} [v]_K + \frac{1}{Z_C} \sum_{k=1}^{\infty} \alpha_k (a_k + b_k) C_{kK} \tag{68}$$

Orthogonality used for matching of vorticity gives

$$\alpha_k^2 b_k = -Ha^{-1} [\omega]_k + \frac{1}{Z_C - Z_c} \sum_{K=1}^{\infty} \alpha_K^2 B_K C_{kK}, \tag{69}$$

where

$$[\omega]_k = \frac{1}{Z_C - Z_c} \int_{Z_c}^{Z_C} [\omega] \sin(\beta_k (z - Z_c))\, dz. \tag{70}$$

The last condition results in

$$\alpha_k^3 (a_k - b_k) = \frac{1}{Z_C - Z_c} \sum_{K=1}^{\infty} \alpha_K^3 (A_K - B_K) C_{kK}. \tag{71}$$

We may summarize as follows:

$$\begin{array}{rcrcl} A_K & = & [\phi]_K & + & \frac{1}{Z_C} \sum a_k C_{kK} \\ \alpha_K (A_K + B_K) & = & Ha^{-1/2} [v]_K & + & \frac{1}{Z_C} \sum \alpha_k (a_k + b_k) C_{kK} \\ \alpha_k^2 b_k & = & -Ha^{-1} [\omega]_k & + & \frac{1}{Z_C - Z_c} \sum \alpha_K^2 B_K C_{kK} \\ \alpha_k^3 (a_k - b_k) & = & & & \frac{1}{Z_C - Z_c} \sum \alpha_K^3 (A_K - B_K) C_{kK} \end{array} \tag{72}$$

We clearly see that the problem is mainly governed by core potentials and that the corrections due to core velocity and vorticity become unimportant as $Ha \to \infty$. The

solution of the problem is obtained by an iterative process. Initially $a_k = b_k = 0$ is assumed and first estimates of A_K and B_K are calculated. Then b_k and a_k are updated and a better approximation for A_K and B_K is obtained. This procedure is repeated (with underrelaxation if necessary) until A_K, B_K and a_k, b_k approach their final constant values.

For the calculations of the coefficients we must evaluate the integrals introduced above. With

$$\tfrac{1}{2}[\omega] = [v] = 4[\phi] = \begin{cases} \frac{Z_C - z}{Z_C - Z_c} & \text{for} \quad Z_c < z < Z_C \\ 1 & \text{for} \quad 0 < z < Z_c \end{cases} \tag{73}$$

we find for potentials

$$\begin{aligned} [\phi]_K &= \frac{2}{Z_C}\left(\int_0^{Z_c}\left(\frac{1}{4}\right)\cos(\beta_K z)\,dz + \int_{Z_c}^{Z_C}\left(\frac{1}{4}\frac{Z_C - z}{Z_C - Z_c}\right)\cos(\beta_K z)\,dz\right) \\ &= \frac{1}{2}\frac{\cos\beta_K Z_c}{Z_C(Z_C - Z_c)\beta_K^2} \end{aligned} \tag{74}$$

and velocity

$$[v]_K = 4[\phi]_K\,. \tag{75}$$

The expansion of vorticity reads

$$\begin{aligned} [\omega]_k &= \frac{1}{Z_C - Z_c}\int_{Z_c}^{Z_C}[\omega]\sin(\beta_k(z - Z_c))\,dz \\ &= \frac{2}{Z_C - Z_c}\frac{1}{\beta_k}, \end{aligned} \tag{76}$$

and the coefficients become

$$\begin{aligned} C_{kK} &= 2\int_{Z_c}^{Z_C}\sin(\beta_k(z - Z_c))\cos(\beta_K z)\,dz \\ &= 2\beta_k\frac{\cos\beta_K Z_c}{\beta_k^2 - \beta_K^2}. \end{aligned} \tag{77}$$

A.2 Lid driven rotating flows

Finally it should be noted, that the present analysis applies also well to a flow problem that recently has been studied by Kharicha, Alemany and Bornas (2004). The latter authors consider the MHD flow in a cylindrical container where an entire end-wall is rotating. They assume that the rotating wall is perfectly electrically connected with the wall tangent to the magnetic field. This yields a reference value for electric potential as $\phi_0 = -\frac{1}{2}$. The fluid domain ends now at $x = 0$ ($r = 1$) and the boundary conditions at this wall are $\phi = 0$, $v = 0$. Therefore all A_K and B_K vanish identically. The core potential has the solution

$$\phi_c = \frac{1}{2}\left(r^2 - 1\right)\left(1 - \frac{z}{Z_C}\right) \tag{78}$$

and it is identical to the wall potential at $x = 0$. This results in $[\phi] = 0$ and as a consequence all a_k which are derived from (58) as

$$\sum_{k=1}^{\infty} a_k \sin \beta_k z = -\left[\phi\right], \quad \text{where } \beta_k = \frac{k\pi}{Z_C}, \tag{79}$$

must vanish. Since $A_K = B_K = a_k = 0$, there remain only the coefficients b_k which have to be determined.

The solution for core velocity becomes

$$v_c = r\left(1 - \frac{z}{Z_C}\right) \tag{80}$$

and it determines the values of

$$[v] = 1 - \frac{z}{Z_C}. \tag{81}$$

The equation (59) that determines now the coefficients b_k reads

$$\sum_{k=1}^{\infty} \alpha_k \left(a_k + b_k\right) \sin \beta_k z = -Ha^{-1/2}\left[v\right] \tag{82}$$

and it yields finally

$$Ha^{1/2}\alpha_k b_k = -\frac{2}{Z_C \beta_k}. \tag{83}$$

A comparison of results for circumferential velocity

$$v = v_c - \frac{2}{Z_C}\sum_{k=1}^{\infty} \frac{\sin \beta_k z}{\beta_k} \tag{84}$$

with those published by Kharicha et al. (2004) and Bessaih, Marty and Kadja (1999) gives perfect agreement as shown in Fig. 12. We observe in the center the solid body type of rotation. Approaching the tangent wall the velocity exceeds the speed of solid body rotation before it decreases in order to satisfy no-slip at the wall.

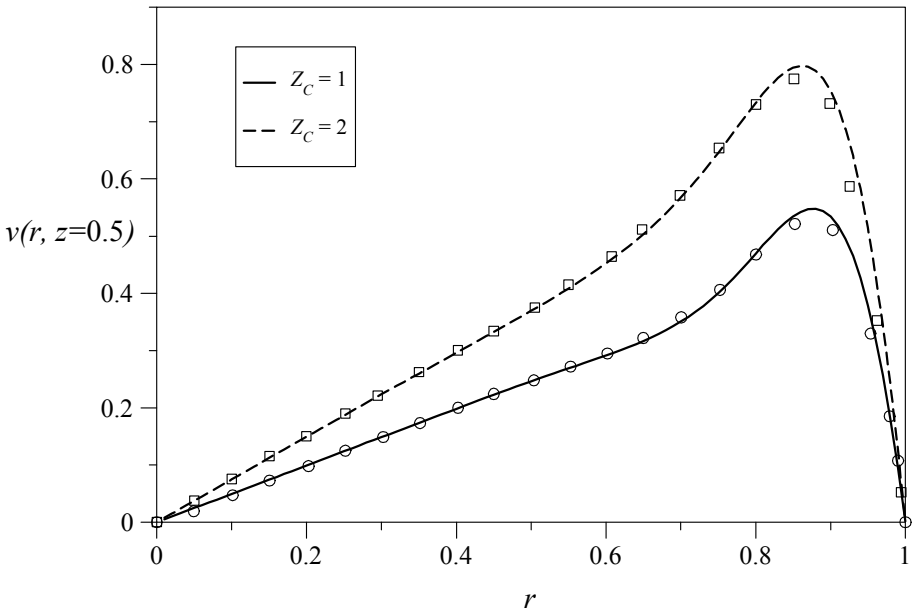

Figure 12: MHD flow in a cylinder driven by a rotating bottom wall at $Ha = 100$. Circumferential velocity $v\,(r, z = 0.5)$ for a cylinder with $Z_C = 1$, and 2. The symbols denote the numerical solution obtained by Kharicha et al. (2004).

References

Antimirov, M. Y. and Molokov, S. Y.: 1989, Magnetohydrodynamic flow in the rotation of a disk in a strong magnetic field, *Magnetohydrodynamics* **25**(1), 71–76.

Bessaih, R., Marty, P. H. and Kadja, M.: 1999, Numerical study of disc driven rotating MHD flow metal in a cylindrical enclosure, *Acta Mechanica* **135**, 153–167.

Bühler, L.: 2003, Inertialess magnetohydrodynamic flow in expansions and contractions, *Technical Report FZKA 6904*, Forschungszentrum Karlsruhe.

Dormy, E., Jault, D. and Soward, A. M.: 2002, A super-rotating shear layer in magnetohydrodynamic spherical couette flow, *Journal of Fluid Mechanics* **452**, 263–291.

Fidaros, D.: 2004, Numerical simulation of rotating magnetohydrodynamic flows, *Technical report*, University of Thessaly.

Hollerbach, R. and Skinner, S. .: 2001, Instabilities of magnetically induced shear layers and jets, *Proceedings of The Royal Society London* **457**(2008), 785–802.

Hunt, J. C. R. and Malcolm, D. G.: 1968, Some electically driven flows in magnetohydrodynamics. Part 2. Theory and experiment, *Journal of Fluid Mechanics* **33**(4), 775–801.

Hunt, J. C. R. and Stewartson, K.: 1969, Some electically driven flows in magnetohydrodynamics. Part 3. The asymptotic theory for flow between circular electrodes, *Journal of Fluid Mechanics* **38**(2), 225–242.

Kharicha, A., Alemany, A. and Bornas, D.: 2004, Influence of the magnetic field and the conductance ratio on the mass transfer rotating lid driven flow, *International Journal of Heat and Mass Transfer* **47**(8-9), 1997–2014.

Lehnert, B.: 1952, Experimrnts on non-laminar flow of mercury in presence of a magnetic field, *Tellus* **4**, 63–67.

Lehnert, B.: 1956, An instability of laminar flow of mecury caused by an external magnetic field, *Proc. Roy. Soc. Lond.* **233**, 299–301.

Molokov, S.: 1993, Single-component magnetohydrodynamic flows in a strong uniform magnetic field. 2. Rotation of an axisymmetric body, *Magnetohydrodynamics* **29**(2), 175–180.

Moreau, R.: 1990, *Magnetohydrodynamics*, Kluwer Academic Publisher.